# External field effects on the resonant frequency of magnetically capped oscillators for magnetic resonance force microscopy

Casey W. Miller,[a] Utkur M. Mirsaidov, Troy C. Messina, Yong J. Lee, and John T. Markert[b]
*Department of Physics, University of Texas, Austin, Texas 78712*

(Presented on 12 November 2002)

We study the resonant frequency shift of CoPt-capped single-crystal-silicon micro-oscillators when a magnetic field is applied perpendicular to the magnetic film, as required for application to nuclear magnetic resonance force microscopy. The oscillator resonant frequencies show two distinct regimes of behavior. At low fields, when the magnetic moment is nearly perpendicular to the external field, the frequency decreases sharply with field, while at high fields, when the moment and field are nearly aligned, the frequency increases. We present models that accurately describe both behaviors. The transition point between these two regimes scales with the volume of the micromagnets. © *2003 American Institute of Physics.* [DOI: 10.1063/1.1557351]

Magnetic resonance force microscopy (MRFM) has advanced quite rapidly since its proposal by Sidles in 1991,[1–5] with most work performed in the sample-on-oscillator configuration. The eventual practical use of MRFM for biological and solid state imaging, however, is heavily dependent upon the successful conversion to the magnet-on-oscillator configuration. This configuration is often implemented with the external polarizing magnetic field, $H_0$, parallel to the cantilever axis in order to minimize the interaction of the field with the magnetic particle.[6,7] In this work, however, $H_0$ is normal to the face of the oscillator; this arrangement is convenient for operation in small bore (1.5 in. diam) superconducting magnets, as the axis of the interferometer optical fiber can then be parallel to the axis of the bore. This configuration is also beneficial because it offers a convenient field gradient geometry for MRFM image deconvolution (irregular magnet geometries[6] can provide force maps that are less straightforward to interpret). The ultimate goal for simple image deconvolution is to use small circular ferromagnetic films to supply a well defined local field gradient.

The general experimental setup for a magnet-on-oscillator MRFM experiment is shown in Fig. 1(a). The magnet on the oscillator generates a field gradient $\nabla B$ in the otherwise homogenous field $H_0$. In the presence of this field gradient, the magnetization $\mathbf{M}$ of the sample imposes a force on the mechanical oscillator equal to $(\mathbf{M}\cdot\nabla)\mathbf{B}$. A frequency-modulated magnetic field is introduced using a radio frequency coil to manipulate the spins of the sample in such a way that a thin slice of the magnetization, and thus the force on the oscillator, becomes a function of time. By cyclically inverting this magnetization at the resonant frequency of the oscillator, a vibration amplitude is detected using a fiber optic interferometer. The force sensitivity is limited by the thermal noise of the mechanical oscillator, $F_{\min}=\sqrt{4k_bTk_0\Delta\nu/Q\omega_0}$, where $k_0$, $\omega_0$, and $Q$ are the spring constant, resonant frequency, and quality factor of the oscillator, and $\Delta\nu$ is the equivalent noise bandwidth of the measurement. Typical oscillators fabricated in our lab are 200 nm thick, have spring constants ~0.01 N/m, resonant frequencies ~10 kHz, and quality factors $\sim 10^3$, resulting in a nominal room temperature force sensitivity on the order of $10^{-15}\,\mathrm{N}/\sqrt{\mathrm{Hz}}$.

The dimensions of the CoPt micromagnets discussed in this work are presented in Table I, and schematics of the two types of oscillators used are given in Fig. 1(b). The CoPt source was produced by arc melting stoichiometric mixtures of Co (99.9975% pure) and Pt (99.9999% pure) in a water-cooled copper hearth in a zirconium-gettered inert atmo-

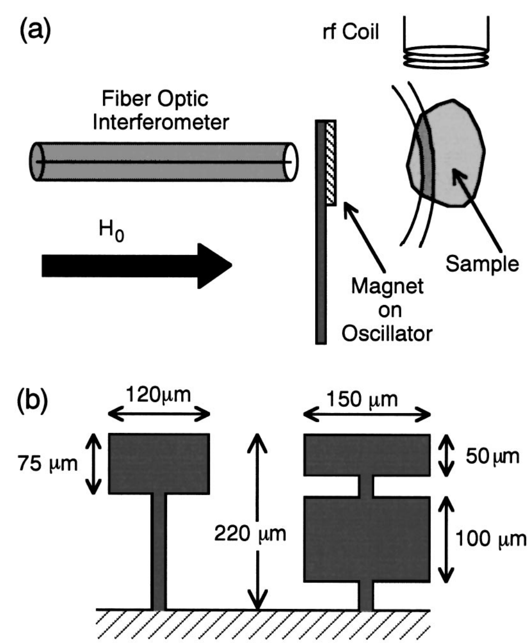


FIG. 1. (a) General MRFM experimental setup with the magnetic film deposited on the mechanical oscillator. (b) Dimensions of the paddles and double torsional oscillators. The oscillators are 200 nm thick, and the necks are 15 $\mu$m wide.

[a]Electronic mail: cmiller@physics.utexas.edu
[b]Author to whom correspondence should be addressed.

TABLE I. CoPt magnetic film dimensions and oscillator data.

| Oscillator | $\omega_0(0)/2\pi$ (kHz) | 1 ($\mu$m) | $w$ ($\mu$m) | $t$ (nm) |
|---|---|---|---|---|
| $A$ | 6.545 | 120 | 10 | 80 |
| $B$ | 10.497 | 150 | 20 | 80 |
| $C$ | 5.840 | 120 | 75 | 80 |

sphere. The single crystal silicon oscillators were then shadow masked and placed in the vacuum chamber with a base pressure of $10^{-8}$ Torr. CoPt films were deposited using electron-beam evaporation; a quartz resonant growth monitor measured a thickness of $80\pm1$ nm.

To determine the effect of $H_0$ on the magnet-capped oscillators, room temperature frequency scans were performed in an exchange gas pressure of 100 mTorr for magnetic fields between $-5$ and $+5$ T. The oscillators were glued to a piezo plate that applied a sinusoidal driving force. The vibration amplitude of the oscillators was detected using a fiber optic interferometer operating at 660 nm. For each of the oscillators discussed here, the first cantilever mode was utilized, as verified by phase-sensitive detection on opposite sides of the oscillator heads.[8,9] The resonant frequencies $\omega_0$ were determined by fitting the vibration amplitude to a Lorentzian. $H_0$ was changed from $+5$ to $-5$ T and back to $+5$ T for each oscillator to investigate hysteresis, though none was detected.

The frequency shifts normalized to the zero field frequency of the magnet-capped oscillators and one bare paddle are shown in Fig. 2. The initial frequency shift of the bare oscillator is attributed to the paramagnetism of the heavily boron-doped single-crystal silicon. Note that the resonant frequency of the silicon paddles exhibit negligible field dependence in the high-field region of interest for MRFM. The magnet-capped oscillators exhibit two regimes of $H_0$ dependence. The low-field behavior occurs while the strong shape anisotropy of the films confines the moment to the plane of the oscillator, and thus nearly perpendicular to $H_0$. The high-field behavior occurs when the field is strong enough to rotate the moment out of the plane, nearly aligned with $H_0$. Although the frequency increases at high fields, it never fully recovers to the zero-field frequency. This can be beneficial to MRFM experiments because lower oscillator frequencies help to meet the adiabatic condition for adiabatic inversion[10] of sample spins. The extreme shifts in frequency for low fields, however, could pose serious problems for experiments limited in field strength or that use modulated external fields.

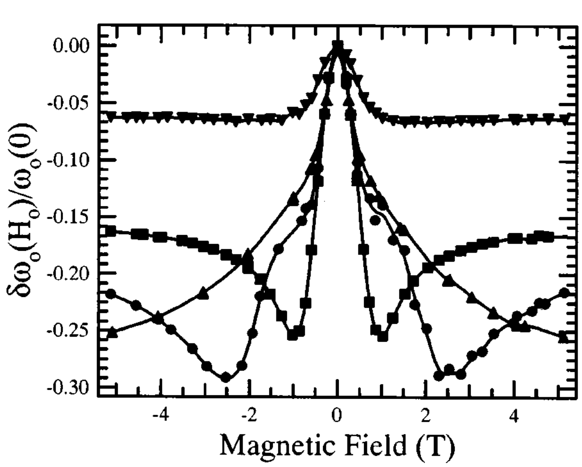


FIG. 2. Normalized shift in resonant frequency for a bare paddle (▼), and magnetically capped oscillators $A$ (■), $B$ (●), and $C$ (▲). The shoulder in the data for oscillator $B$ may be due to a shift of the in-plane easy axis. The lines are guides to the eye.

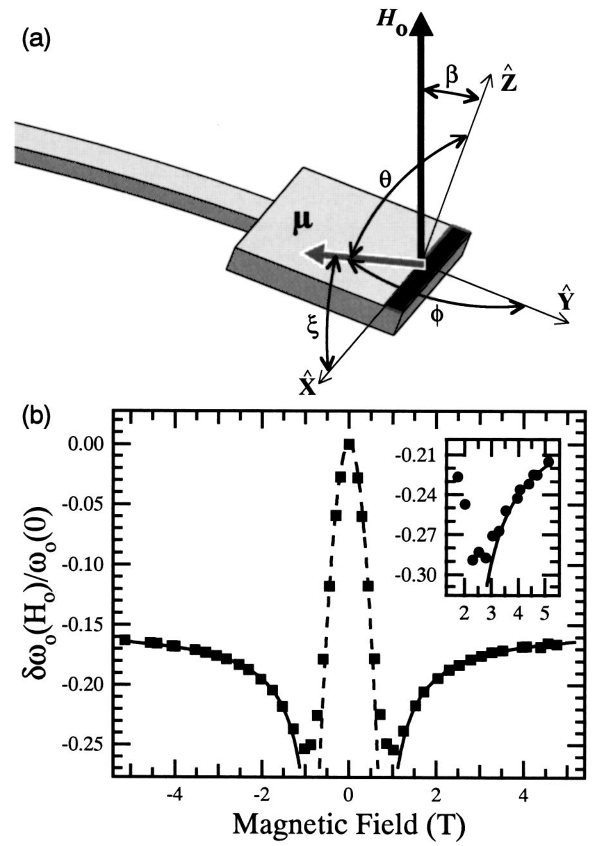


FIG. 3. (a) Illustration of the coordinates, parameters and geometry used for the low-field model of Eq. (2). (b) Oscillator $A$ data with fits to Eq. (2) in the low-field regime (dashed) to Eq. (1) in the high-field regime (solid). The inset is data from oscillator $B$ with a fit to Eq. (1) for high fields.

The field dependence seen in the high-field regime is similar to that previously reported for the geometry where $H_0$ is in the plane of the oscillator.[6] The increase in resonant frequency with $H_0$ is due to an increase in the effective spring constant that is caused by the small restoring torque that is present. When the moment and $H_0$ are aligned, such magnetic stiffening causes a shift in the resonant frequency equal to

$$\frac{\Delta\omega_0}{\omega_0}=\frac{\mu H_0}{2k_0L_{\mathrm{eff}}^2}\frac{H_k}{(H_0+H_k)}, \tag{1}$$

where $\mu$ is the magnetic moment, $H_k$ is the anisotropy field, and $L_{\mathrm{eff}}$ is the effective length of the cantilever. Figure 3 shows the data for oscillators $A$ and $B$ fit to Eq. (1) with the substitution $H_0\rightarrow H_0+H_s$, where $H_s$ is an offset field above which the moment and $H_0$ are nearly aligned and the small angle approximation validates this model. The physical interpretation of $H_s$ is not clear, but may be related to domain processes. A least squares fit allows us to determine $\mu$, $H_k$, and $H_s$ of oscillators $A$ and $B$ to be $\mu^{(A)}=7.1\times10^{-11}$ J/T, $H_K^{(A)}=0.61$ T, $H_s^{(A)}=1.21$ T, and $\mu^{(B)}=1.6\times10^{-10}$ J/T, $H_K^{(B)}=0.69$ T, $H_s^{(B)}=2.27$ T, respectively. The moment values are in good agreement with those estimated from the saturation magnetization[11] (750 kA/m) and magnet volumes ($\mu^{(A)}\approx7.2\times10^{-11}$ J/T, $\mu^{(B)}\approx1.6\times10^{-10}$ J/T).

This model, however, cannot explain the effects observed in the low-field regime. The model we propose for the low-field behavior considers the magnetic energy in the three primary directions of the film. We model the magnetization of the film as a single domain that initially lies in the $x$ direction and that is confined to the $x-z$ plane. Further, we assume the oscillations of the cantilever occur in the $y-z$ plane. The energy is written as the sum of anisotropy and Zeeman energy terms, $E=(K_X\sin^2\xi+K_Y\sin^2\phi+K_Z\sin^2\theta)V-MH_0V(\cos\beta\cos\theta-\sin\beta\cos\phi)$, where $\xi$, $\phi$, and $\theta$ are the angles from the primary axes of the micromagnet to the magnetic moment direction, $\beta$ is the tilt angle of the cantilever with respect to $H_0$, and $K_i$ is the anisotropy constant in the $i$th principle direction, as depicted in Fig. 3(a). Minimizing the energy with respect to $\theta$ yields $\cos\theta=-H_0/H_{k(z,x)}$, where $H_{k(z,x)}=2(K_z-K_x)/M$. The $x$ component of the restoring torque, given by $\tau_x=\mu H_0^2\beta/H_{k(z,x)}$, induces a change in the spring constant of $\Delta k_0=\tau_x/\beta L_{\mathrm{eff}}^2$. For small changes $\Delta\omega_0/\omega_0=\Delta k_0/(2k_0)$, so we find the normalized frequency shift for low fields to be

$$\frac{\Delta\omega_0}{\omega_0}=\frac{-\mu H_0^2}{2k_0L_{\mathrm{eff}}^2}\left(\frac{1}{H_{k(z,x)}}\right). \tag{2}$$

This model reduces to the high-field model with appropriate assumptions.

Figure 3(b) shows the normalized frequency shift for oscillator $A$ with a least squares fit to Eq. (2). The fit yields $H_{k(z,x)}=-0.27$ T, where we have used the magnetic moment from the high-field fit. The sign and magnitude of the composite anisotropy field factor shows the preference of the moment to lie in the plane of the film.

The transition between regimes is marked by a sharp minimum that reflects the energy necessary to overcome the shape anisotropy of the thin films. For our films with similar dimensions this energy scales with the volume of the micromagnets; the minima correspondingly shift with volume. The volume ratios $V_A:V_B:V_C$ are 1:2.3:7.5. This is in good agreement with the observed minima; the transition point for oscillator $A$ is approximately 1.0 T, and that for oscillator $B$ is around 2.3 T, while no transition is detected for oscillator $C$ for field strengths below 5.0 T. These transition points correspond well to the $H_s$ values from the fit of the high-field data to Eq. (1).

The shift in resonant frequency of single-crystal-silicon oscillators with magnetic films of various sizes has been observed to exhibit two regimes of response to a perpendicular external field at room temperature. The low-field regime is characterized by a sharp decrease in resonant frequency with applied field, in agreement with our simple anisotropy-based model. The increase in resonant frequency for high fields is consistent with previous results. The transition point between regimes scales with the volume of the magnets. A dynamical model that describes both regimes and the transition will be presented in a future publication.[12] This work suggests high-field magnet-on-oscillator MRFM experiments can be performed in the perpendicular configuration without significant complications, although low-field experiments may encounter difficulties due to the drastic frequency shifts observed in this regime.

The authors thank Michelle Chabot for fabricating the oscillators, and Enrico Rossi for theory discussions. This work was supported by Army Research Office Contract No. DAAD-19-02-C-0064, National Science Foundation Grant No. DMR-0072365, and The Robert A. Welch Foundation Grant No. F-1191.


1. J. A. Sidles, Appl. Phys. Lett. **58**, 2854 (1991).
2. B. C. Stipe, H. J. Mamin, C. S. Yannoni, T. D. Stowe, T. W. Kenny, and D. Rugar, Phys. Rev. Lett. **87**, 277602 (2001).
3. Z. Zhang and P. C. Hammel, IEEE Trans. Magn. **33**, 4047 (1997).
4. J. A. Mahron, R. Fainchtein, and D. D. Smith, J. Appl. Phys. **86**, 4619 (1999).
5. O. Klein, V. V. Naletov, and H. Alloul, Eur. Phys. J. B **17**, 57 (2000).
6. B. C. Stipe, H. J. Mamin, T. D. Stowe, T. W. Kenny, and D. Rugar, Phys. Rev. Lett. **86**, 2874 (2001).
7. J. A. Mahron, R. Fainchtein, and D. D. Smith, Appl. Phys. Lett. **73**, 3778 (1998).
8. M. D. Chabot and J. T. Markert, Proc. SPIE **3875**, 104 (1999).
9. M. D. Chabot, T. C. Messina, V. Mancevski, C. W. Miller, and J. T. Markert, Proc. SPIE **4559**, 24 (2001).
10. K. Wago, D. Botkin, C. S. Yannoni, and D. Rugar, Phys. Rev. B **57**, 1108 (1998).
11. Y. Yamada, T. Suzuki, and E. N. Abarra, IEEE Trans. Magn. **33**, 3622 (1997).
12. E. M. Rossi, C. W. Miller, U. M. Mirsaidov, A. H. MacDonald, and J. T. Markert (unpublished).